Supporting Information

Fe-doped Ni_3S_2/NiS heterojunction with improved electrocatalytic activity and stability for alkaline oxygen evolution reaction

Jiening Sun,[a] Licheng Miao*[b], Zhichuan J.Xu[c], and Zhipeng Sun*[a b]

[a] School of Materials and Energy, Guangdong University of Technology, Guangzhou, 510006, Guangdong, China. zpsunxj@gdut.edu.cn (Z. Sun).

[b] Key Laboratory of Advanced Energy Materials Chemistry (Ministry of Education), College of Chemistry, Nankai University, Tianjin 300071, China, miaolicheng@126.com.

[c] School of Material Science and Engineering, Nanyang Technological University, Singapore, 639798, Singapore.

1. Computational details

Density functional theory (DFT) calculations were conducted using the Vienna Ab Initio Simulation Package (VASP).[1] The electron-ion and electron-electron interactions were modeled with projector-augmented wave (PAW) pseudopotentials and Perdew-Burke-Ernzerhof (PBE) exchange and correlation functionals, respectively.[2,3] A 4×3×1 k-point grid and an energy cut-off of 450 eV were utilized in all computations. Energy convergence was set at 10^{-5} eV and the atomic force criterion at 0.02 eV $Å^{-1}$ to ensure full relaxation of atomic positions. A 20 Å vacuum layer was included between the two sheets to prevent interlayer interactions. Spin-polarized calculations were employed for all systems. Solvation effects were accounted for using an implicit solvation model, VASPsol, with default settings of 78.4 for the dielectric constant, 0.6 for the width of the dielectric cavity, and 0.525 meV $Å^{-2}$ for the dielectric cavity surface tension.[4] Free energy corrections for intermediate species were carried out with VASPKIT.[5] The free energy of gas-phase O_2 ($G[O_2]$) was derived from

$$G[\mathrm{O_2}] = 4.92(\mathrm{eV}) + 2G[\mathrm{H_2O}] - 2G[\mathrm{H_2}]$$

by using the experimental Gibbs free energy of the reaction $2H_2O(l) \rightarrow O_2(g) + 2H_2(g)$ in standard conditions. Visualization and analysis of the figures were conducted using VESTA.

2. Materials preparation

Weigh 5 mg of RuO_2 to form a uniform ink with Nafion binder and 980 μL of

dispersant (isopropanol to water ratio of 9:1).[6] The obtained suspension was sonicated for 30 min to obtain a uniform ink. Then apply it on foam nickel and place it for 12h to dry the working electrode. The test area is 0.5 cm^2 and the load capacity is 4.3 mg cm^{-2}.

3. Material characterization

The crystal structure of the difference catalyst was characterized by an X-ray diffractometer (XRD, Ultima-IV, Cu Kα radiation) with the 2θ ranges from 10° to 80° at a scanning rate of 10°/min. SEM (SU8010) and TEM characterized the catalyst's microstructure and element composition. The X-ray photoelectron spectroscopy (XPS) was recorded on a Thermo Scientific Nexsa with an Al Kα source. The nickel foam was cut to 5 mm × 5 mm without any special surface treatment. The XPS spectrums were analyzed and fitted by Themo Avantage software. All the tested binding energies were calibrated to 284.8 eV of the C1s carbon peak.

4. Supporting Figures and Tables

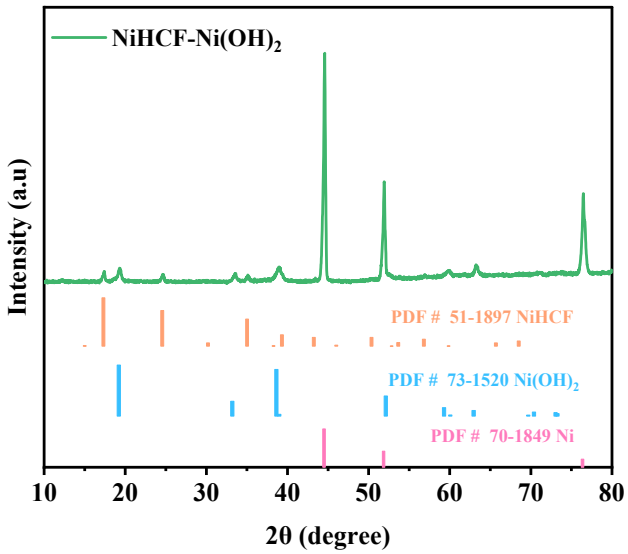

Fig. S1 XRD pattern of NiHCF-$Ni(OH)_2$.

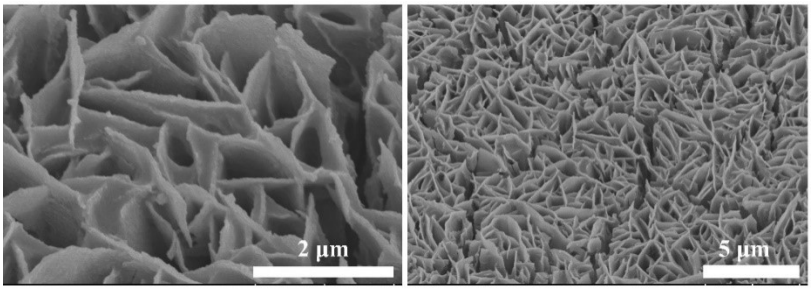

Fig. S2 The SEM of Ni_3S_2/NiS.

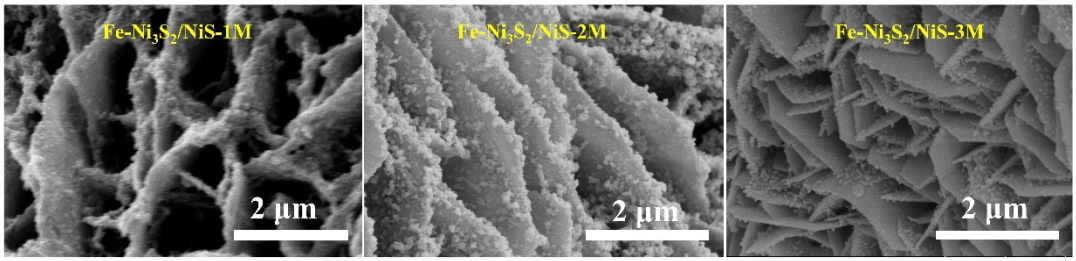

Fig. S3 The SEM of different Na_2S concentrations in Fe-Ni_3S_2/NiS.

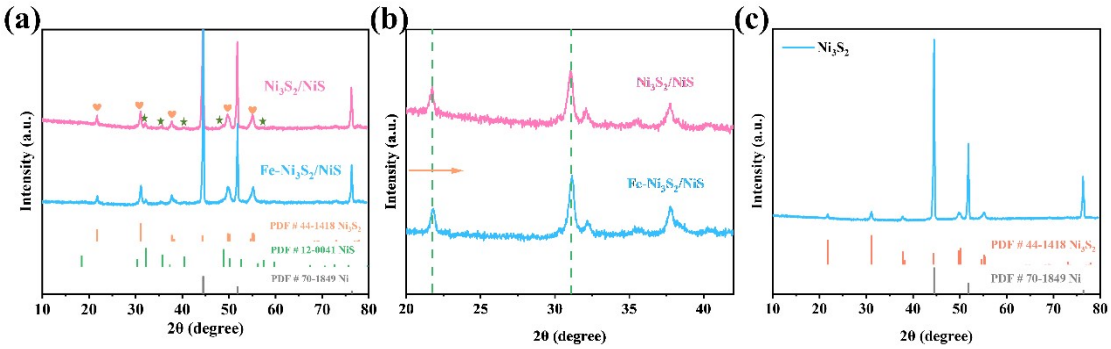

Fig. S4 (a) The XRD pattern of Fe-Ni_3S_2/NiS and Ni_3S_2/NiS. (b) The enlarged XRD plot at 20~40°. (c) The XRD pattern of Ni_3S_2.

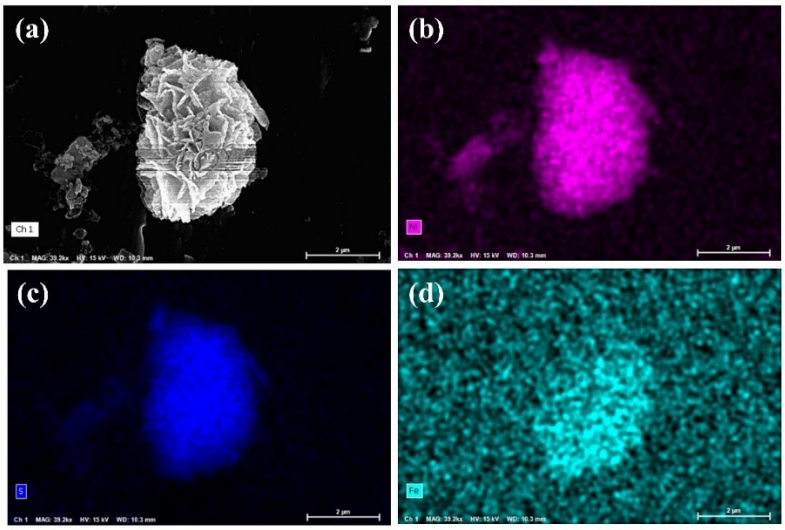

Fig. S5 The EDS of Fe-Ni_3S_2/NiS (the catalyst is sonicated from the Nickel foam for testing).

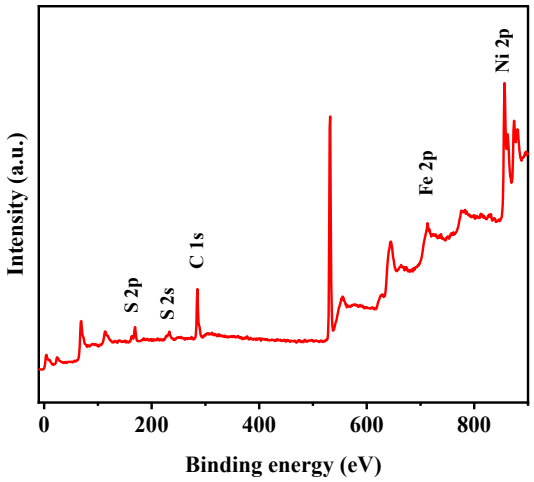

Fig. S6 The survey XPS spectrum of Fe-Ni_3S_2/NiS.

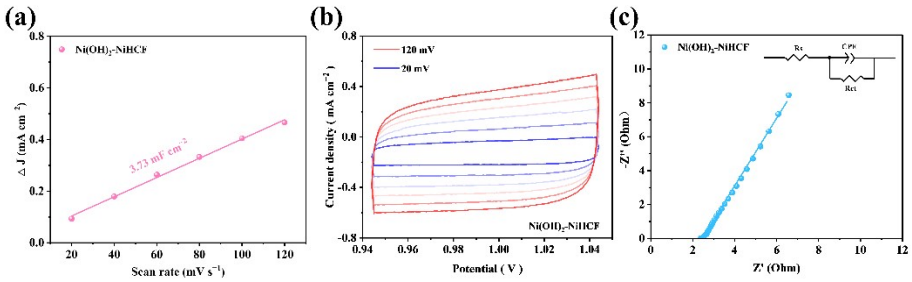

Fig. S7 (a) The C_{dl}, (b) CV curve, and (d) EIS of $Ni(OH)_2$-NiHCF.

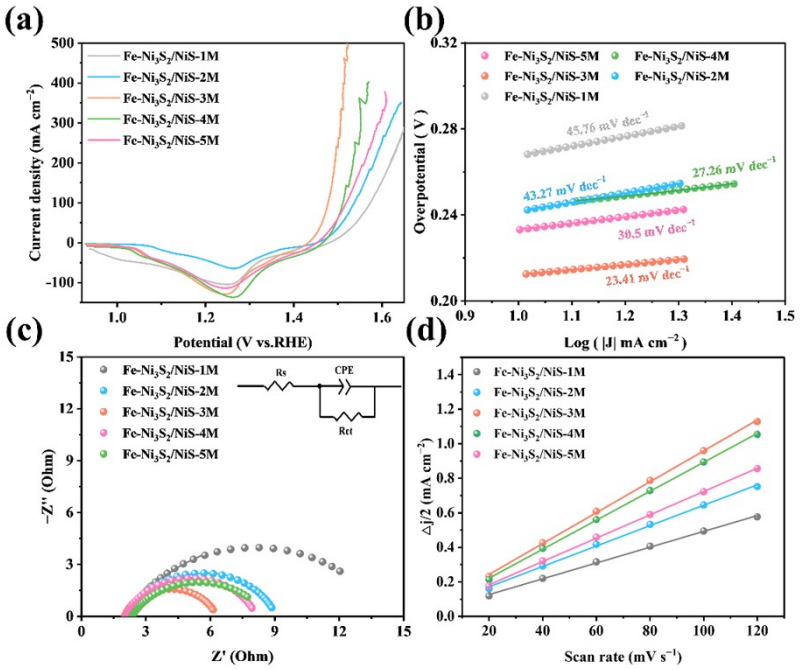

Fig. S8 (a) LSV, (b)Tafel curve, (c) Nyquist with the fitting curves plotted, and (d) C_{dl} of different Na_2S concentration Fe-Ni_3S_2/NiS.

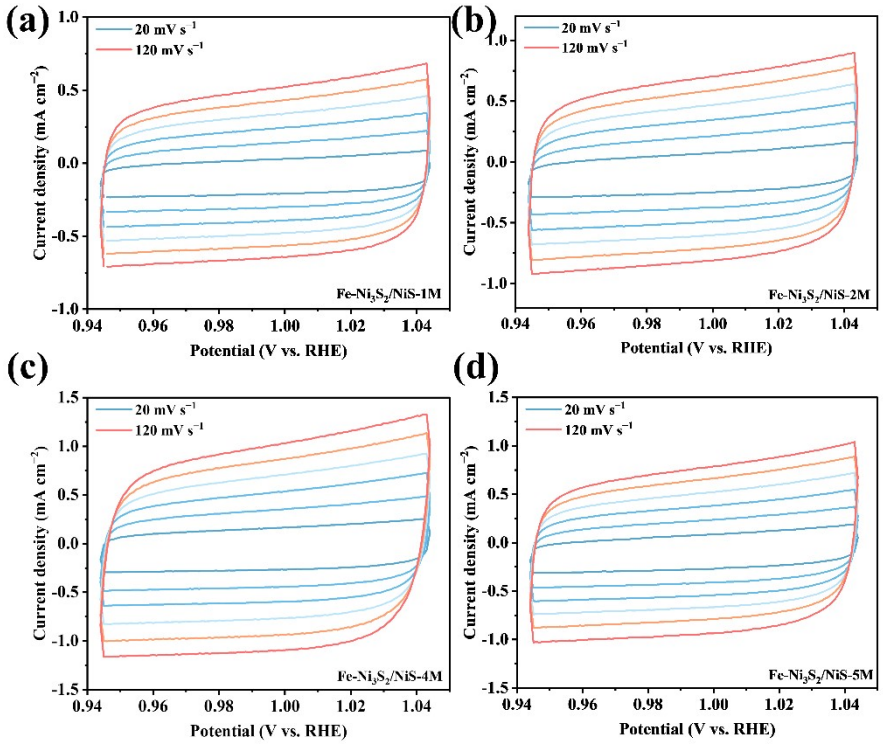

Fig. S9 The CV curve of different scan rates of (a) Fe-Ni_3S_2/NiS-1M, (b) Fe-Ni_3S_2/NiS-2M, (c) Fe-Ni_3S_2/NiS-4M, and (d) Fe-Ni_3S_2/NiS-4M.

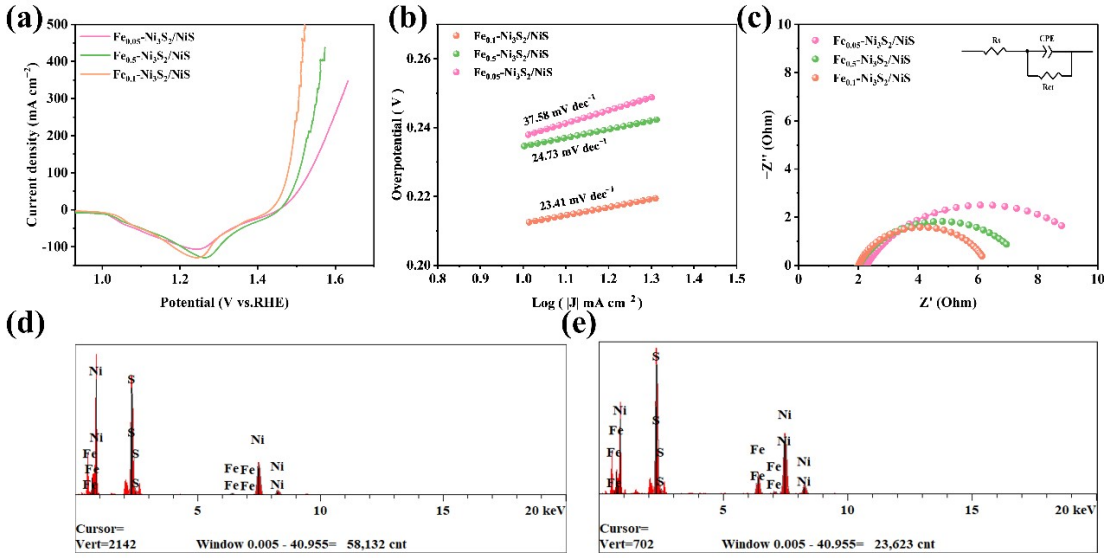

Fig. S10 (a) IR-corrected polarization curves, (b) Tafel slope, and (c) EIS of $Fe_{0.05}$-Ni_3S_2/NiS, $Fe_{0.5}$-Ni_3S_2/NiS 和 Fe-Ni_3S_2/NiS. The EDS of (d) $Fe_{0.05}$-Ni_3S_2/NiS, (e) $Fe_{0.5}$-Ni_3S_2/NiS (the content of element content is shown in Table 1 and 2, respectively).

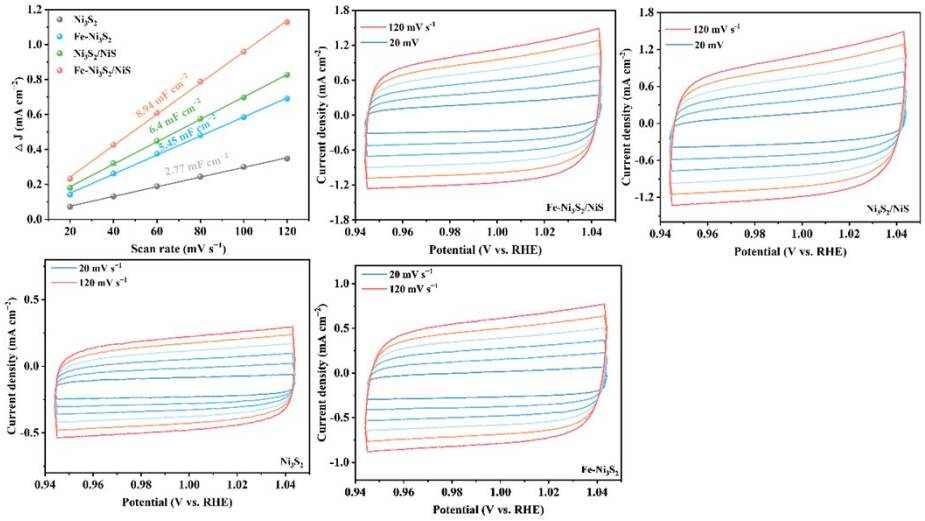

Fig. S11 (a) The calculated Cdl of Ni_3S_2, Fe-Ni_3S_2, Ni_3S_2/NiS and Fe-Ni_3S_2/NiS. The CV curves of (b) Fe-Ni_3S_2/NiS, (c) Ni_3S_2/NiS, (d) Ni_3S_2, and (e) Fe-Ni_3S_2 at different scan rates from 20 to 120 mV s^{-1}.

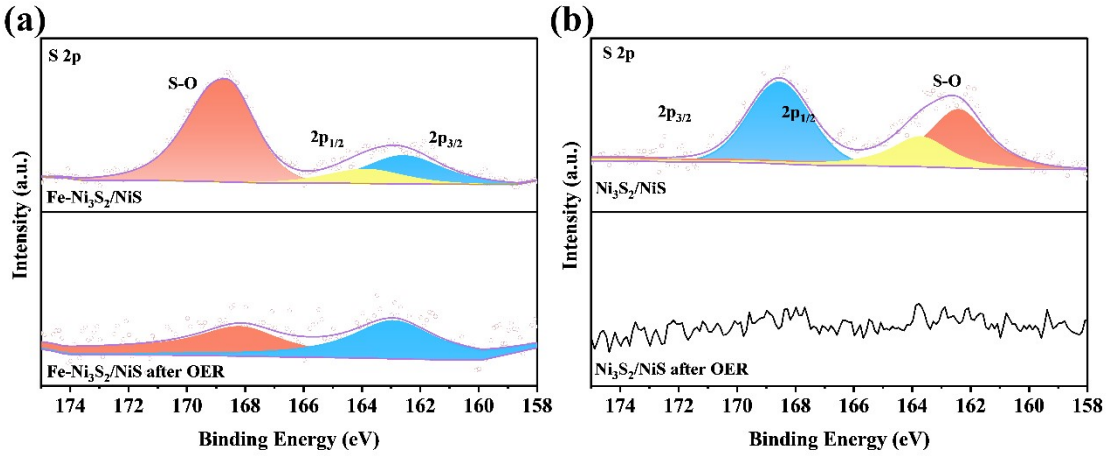

Fig. S12 The XPS spectrum of S 2p: (a) Fe-Ni_3S_2/NiS and (b) Fe-Ni_3S_2 before and after OER.

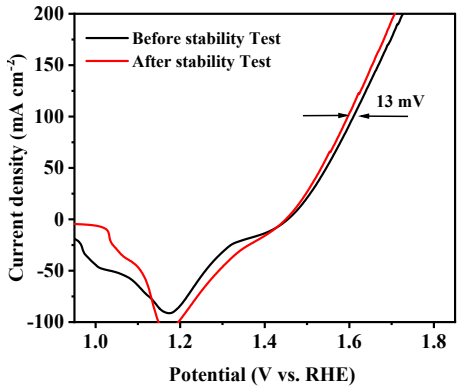

Fig. S13 The LSV curve was compared initially and after OER stability at 500 mA cm^{-2}.

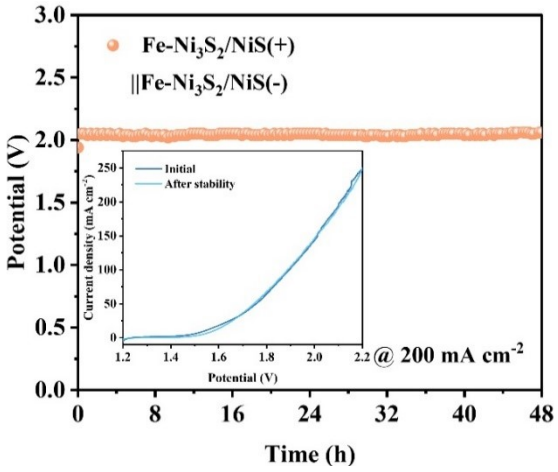

Fig. S14 Chronopotentiometry measurement uses Fe-Ni_3S_2/NiS as the cathode and anode of electrochemical water splitting.

Table. S1 The element content of $Fe_{0.05}$-Ni_3S_2/NiS

Elt.	**Atomic %**	**Conc.**	**Units**	
S	40.883	25.449	wt.%	
Fe	1.663	1.944	wt.%	
Ni	57.454	70.607	wt.%	
	100.000	100.000	wt.%	Total

Table. S2 The element content of $Fe_{0.05}$-Ni_3S_2/NiS

Elt.	**Atomic %**	**Conc.**	**Units**	
S	29.510	18.724	wt.%	
Fe	10.372	11.460	wt.%	
Ni	60.118	69.816	wt.%	
	100.000	100.000	wt.%	Total

Table. S3 The element content of Fe-Ni_3S_2/NiS

Elt.	**Atomic %**	**Conc.**	**Units**	
S	32.02	20.94	wt.%	
Fe	1.92	2.14	wt.%	
Ni	66.07	77.38	wt.%	
	100.000	100.000	wt.%	Total

Table. S4 The element content of Ni_3S_2/NiS after OER

Elt.	Atomic %	Conc.	Units	
S	0.975	0.535	wt.%	
Ni	99.025	99.465	wt.%	
	100.000	100.000	wt.%	Total

[1] G. Kresse, J. Hafner, Ab initiomolecular dynamics for liquid metals, *Phys. Rev. B.,* 1993, **47**, 558-561.

[2] G. Kresse, D. Joubert, From ultrasoft pseudopotentials to the projector augmented-wave method, *Phys. Rev. B.,* 1999, **59**, 1758-1775.

[3] J.P. Perdew, K. Burke, M. Ernzerhof, Generalized gradient approximation made simple, *Phys. Rev. Lett.,* 1996, **77**, 3865-3868.

[4] Mathew, K.; Sundararaman, R.; Letchworth-Weaver, K.; Arias, T. A.; Hennig, R. G. Implicit solvation model for density-functional study of nanocrystal surfaces and reaction pathways. *J. Chem. Phys.,* 2014, **140**, 084106.

[5] V. WANG, N. XU, J.-C. LIU, G. TANG, W.-T. GENG, VASPKIT: A user-friendly interface facilitating high-throughput computing and analysis using VASP code, *Comput. Phys. Commun.,* 2021, **267**, 108033.

[6] X. Xu, S. Zhang, Q. Zhang, S. Chen, Y. Wu and Z. Sun, Fe-doped and carbon composite multiphase hetero-structured catalysts based on the ion-exchange strategy for seawater electrolysis, *ACS Sustainable Chem. Eng.,* 2023, **11**, 15338-15349.